*R*esearch in
*A*stronomy and
*A*strophysics

Multi-band optical variability of BL Lac object OQ 530 *

Bing-Kai Zhang[1], Ben-Zhong Dai[2], Li Zhang[2] and Zhen Cao[3]

[1] Department of Physics, Fuyang Normal College, Fuyang 236041, China; *zhangbk@ihep.ac.cn*
[2] Department of Physics, Yunnan University, Kunming 650091, China;
[3] Institute of High Energy Physics, Chinese Academy of Sciences, Beijing 100049, China

Abstract   Historical optical data are combined on the BL Lac object OQ 530. Verifying the existence of correlations among the flux variations in different bands serves as an important tool to investigate emission processes. To examine the possible existence of a lag between variations in different optical bands from this source, a statistical analysis is performed through the discrete correlation function (DCF) method and the z-transformed discrete correlation function (ZDCF) method. Monte Carlo simulations called "flux redistribution/random subset selection" (FR/RSS) are performed to obtain statistically meaningful values for the cross-correlation time lags and their related uncertainties. The analysis confirms that the variations in different optical light curves are strongly correlated, with zero-lag within the errors. Long term variability of color indexes is also analyzed. The result suggests a strong correlation between color index and brightness. A clear bluer-when-brighter chromatism is found, in the sense that the spectrum steepens as the brightness decreases.

Key words: BL Lacs: general — BL Lacs: individual (OQ 530)

1 INTRODUCTION

Blazars are the most extreme class of active galactic nuclei (AGNs) in which the relativistic jet is closely aligned with the observer's line of sight (Blandford & Königl 1979; Urry & Padovani 1995). Based on the properties of their optical spectra, blazars are commonly divided into two subclasses: BL Lacertae objects (BL Lacs) and flat spectrum radio quasars (FSRQs). They display double peaked spectral energy distributions (SEDs) which extend from radio up to gamma-rays and sometimes to TeV frequencies. The low-energy peak (radio to UV/X-ray) is generated by synchrotron emission produced by relativistic electrons flowing along the jet, while the high-energy component (extending to gamma-ray) is possibly attributed to inverse Compton emission. Blazars exhibit strong variability at all wavelengths of the whole electromagnetic (EM) spectrum, strong polarization from radio to optical wavelengths, and are usually core dominated radio structures. They vary on diverse time scales (Gupta et al. 2008 and references therein). The study of variability has been one of the most powerful tools in revealing the nature of blazars. Information on variability amplitude, flux variation, lags at different wavelengths, temporal duty cycles, and spectral changes can shed light on the location, size, structure, and dynamics of the non-thermal emitting regions and on the acceleration/radiation

mechanisms (Ciprini et al. 2003). Understanding variation behavior is one of the major issues of AGN studies. In recent years, correlations of the variability in different energy regions have been widely studied (Raiteri et al. 2001, 2008; Dai et al. 2006; Marshall et al. 2008; Arévalo et al. 2008; Chatterjee et al. 2008; Villata et al. 2009; Bonning et al. 2009). It is very significant to search for detectable delays between different optical bands, even if these can be expected to be very small, if any. Optical flux variations in BL Lacs are usually accompanied by changes in the spectral shape. The analysis of spectral changes of blazars can put some strong constraints on the physical processes that are responsible for these variations, and this can be revealed by analyzing color indexes.

OQ 530 was optically identified in 1977 (Kühr 1977) as the counterpart of an extragalactic source included in the NRAO-Bonn radio survey at 5 GHz. Because of its stellar aspect and the faintness of its optical spectral features, it was classified as a BL Lac by Miller (1978). The multifrequency (radio through gamma-ray) spectrum of this source suggests that it is an LBL object (Fossati et al. 1998). The redshift $z = 0.152$ has been determined from absorption features of the host galaxy as well as from [OII] and [OIII] emission lines (Stickel et al. 1991, 1993). Rapid and large amplitude variations for this BL Lacertae object were found by Carini et al. (1990). The intraday optical variability was detected by Heidt & Wagner (1996), while observations over four nights during 1998 June-July showed weak variations on time-scales of weeks (Ghosh et al. 2000). On this source, Liu et al. (2007) found a possible 456-day periodic variation in the optical band. Their result showed no obvious correlation between the optical and radio variations.

The goals in this paper are to investigate the correlations between different optical light curves and to study the variations in color index of this source by collecting available data. The paper is arranged as follows: in Section 2 the historical light curves are presented; then in Section 3 the correlations and the time lags between different optical passbands are reported; the color index is studied in Section 4; the discussion and conclusions are given in Section 5.

2 LIGHT CURVES

The optical light curve of OQ 530 from 1905 until 1977 was derived by Miller (1978) using the Harvard College plate collection. The source showed large-amplitude optical variations on a time scale of days to years, and did not exhibit any obvious periodicity in Miller's study. Barbieri et al. (1982) performed a further study using the Asiago Schmidt plates from 1966 to 1980, and the result suggested the presence of an eclipse phenomenon occurring in this object. A collection of published data until 1993 was published by Fan & Lin (2000). The historic optical light curves of this source showed secular decreasing trends of its mean brightness (Tagliaferri et al. 2003; Massaro et al. 2004).

In this paper, the optical B, V, R and I band data are collected from literatures (Ghosh et al. 2000; Fan & Lin 2000; Massaro et al. 2004). In sum, 1044 data points are compiled. The full light curves of different passbands are displayed in Figure 1. They are very similar, and span more than 25 yr. In order to estimate the total variability of each light curve, the fractional variability amplitude $F_{\rm var}$ is calculated, which is known as

$$F_{\rm var} = \sqrt{\frac{S^2 - \overline{\varepsilon_{\rm err}^2}}{\overline{x}^2}},$$ (1)

where S^2 is the sample variance of the light curve, $\overline{x}$ is the average magnitude and $\overline{\varepsilon_{\rm err}^2}$ is the mean of the squared measurement uncertainties (Edelson et al. 2002; Soldi et al. 2008). The detailed statistics and variabilities of these data are listed in Table 1. The first column is the bands, the second the number of data points, the third the mean values, the fourth the standard deviations, the fifth the largest variations and the last the fractional variability amplitudes.
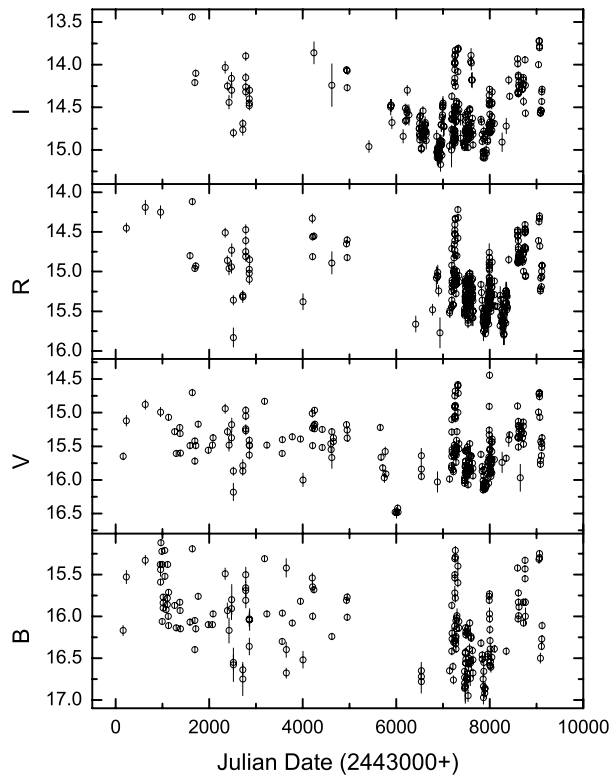
Fig. 1 Light curves of OQ 530 in the $BVRI$ bands.

Table 1 Statistics of Optical Data

Band	N	Mean (mag)	σ (mag)	Δ (mag)	F_{var} (%)
B	188	16.12	0.45	1.85	2.80
V	242	15.55	0.38	2.01	2.42
R	341	15.17	0.36	1.71	2.32
I	273	14.59	0.33	1.73	2.25

3 CORRELATION ANALYSIS

Due to unevenly sampled monitoring data, the discrete correlation function (DCF) method and z-transformed discrete correlation function (ZDCF) method are employed to search for a correlation between the different optical bands.

3.1 Discrete Correlation Function (DCF) Method

The discrete correlation function (DCF) was introduced by Edelson & Krolik (1988). It is a useful method of measuring correlation, and it does not require interpolating in the temporal domain. This method can not only provide the correlation of two series of unevenly sampled variability data with the time lag, but also gives evidence of periods that lie in a single temporal data set. Its other advantages are that it uses all the available data points and calculates a meaningful error estimate. The first

step is to calculate the set of Un-binned Discrete Correlation Functions (UDCF) between each data point in the two data streams. It is defined as follows:

$$\mathrm{UDCF}_{ij} = \frac{(a_i - \overline{a}) \times (b_j - \overline{b})}{\sqrt{\sigma_a^2 \times \sigma_b^2}}, \tag{2}$$

where a_i and b_j are points of the data sets a and b, $\overline{a}$ and $\overline{b}$ are the means of the data sets a and b, and σ_a and σ_b are the standard deviations of each data set. Each of the UDCF values is associated with the pair-wise lag $\Delta t_{ij} = t_j - t_i$. Then we average over the M pairs for which $\tau - \Delta\tau/2 \le \Delta t_{ij} < \tau + \Delta\tau/2$, and obtain the DCF:

$$\mathrm{DCF}(\tau) = \frac{1}{M}\Sigma\mathrm{UDCF}_{ij}(\tau), \tag{3}$$

where M is the number of pairs in the bin. When $a = b$, the autocorrelation DCF is produced, and when $a \ne b$, the cross-correlation DCF is measured. In most cases, the evident peak in the cross-correlation function means a strong correlation between two data series, and the peak in the autocorrelation DCF implies a strong period in the data set. The standard error for each bin is defined as

$$\sigma(\tau) = \frac{1}{M-1}\{\Sigma[\mathrm{UDCF}_{ij} - \mathrm{DCF}(\tau)]^2\}^{1/2}. \tag{4}$$

The standard error is underestimated if one of the series is strongly autocorrelated over widths greater than the bin size, and then the factor $(M - 1)$ in the denominator should be replaced by $[(M - 1)(M' - 1)]^{1/2}$, where M' is the number of uncorrelated UDCF values within the bin. In order to obtain statistically meaningful values for the cross-correlation time lags and their related uncertainties, the common usage is to calculate the centroid τ_c of the DCF, given by

$$\tau_c = \frac{\sum_i \tau_i \mathrm{DCF}_i}{\sum_i \mathrm{DCF}_i}, \tag{5}$$

where sums run over the points which have a DCF value close to the peak one ($\mathrm{DCF}_i > 0.8\mathrm{DCF}_{\mathrm{peak}}$), then perform Monte Carlo simulations known as "flux redistribution/random subset selection" (FR/RSS) described in detail by Peterson et al. (1998) and Raiteri et al. (2003). Random subsets of the two data sets to be tested for correlation are selected, redundant points are discarded, and random gaussian deviations constrained by the flux errors are added to the fluxes. Thus, the influence of both uneven sampling and flux density errors is taken into account. In each simulation, the two subsets are then cross-correlated and the centroid τ_c of the DCF peak is determined. After a large number of simulations (generally 500~2000), the cross-correlation peak (actually, the centroid) distribution (CCPD) is obtained. As the measures of the time lag and its uncertainties, τ_{median} and $\pm\Delta\tau_{68}$ can be computed directly from the CCPD, where $\pm\Delta\tau_{68}$ corresponds to 1σ errors for a normal distribution (Peterson et al. 1998).

3.2 Z-transformed Discrete Correlation Function (ZDCF) Method

Z-transformed discrete correlation function was proposed by Alexander (1997). The ZDCF scheme goes as follows: let n be the number of a_i, b_i pairs in a given time-lag bin. The correlation coefficient is estimated,

$$r = \frac{\sum(a_i - \overline{a})(b_i - \overline{b})}{\sigma_a\sigma_b(n-1)}, \tag{6}$$

where $\overline{a}$, $\overline{b}$ are the estimators of the bin averages, σ_a, σ_b are the standard deviations of each bin. The sampling distribution of r is known to be highly skewed, so it is transformed into Fisher's z:

$$z = \frac{1}{2}\log\left(\frac{1+r}{1-r}\right), \qquad r = \tanh z, \tag{7}$$
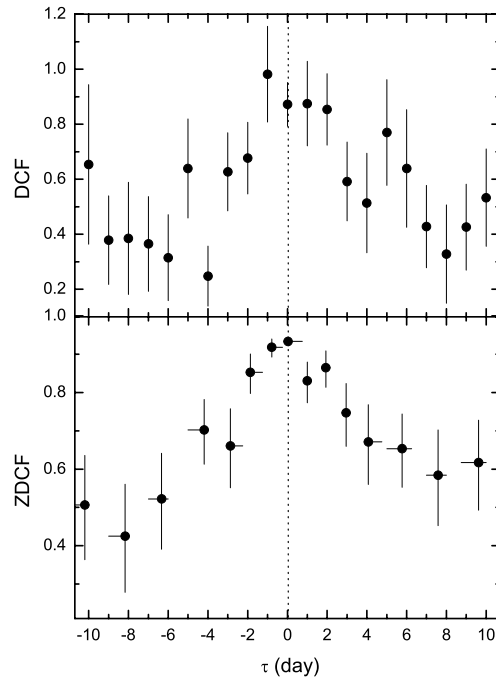
Fig. 2 DCF (*top*) and ZDCF (*bottom*) between the B and V bands.
The dashed vertical line is drawn to guide eyes.

which is an approximately normally distributed random variable with a known mean, $\bar{z}(\rho)$ and variance, $s_z^2(\rho)$. Then the bin's ZDCF is estimated by

$$\mathrm{ZDCF}(\tau) = r_{-(r-\tanh(\bar{z}-s_z))}^{+(\tanh(\bar{z}+s_z)-r)}. \tag{8}$$

The binning is performed according to equal population rather than equal $\Delta\tau$. As a result, the bins are not equal in time-lag width. This method can be considered as an improvement of the DCF technique. Also, it is more robust than the DCF method when applied to very sparse and irregularly sampled light curves (Liu et al. 2008; Roy et al. 2000). The effect of measurement errors is estimated by the Monte Carlo averaged ZDCF of light curves with simulated random errors.

3.3 Result

According to the methods mentioned above, we calculate the DCF and ZDCF between different optical bands to search for correlations and possible time lags. Between the B and V band light curves, the DCF result computed with a bin size of 1 d is shown in the top panel of Figure 2. The curve of the DCF has an obvious maximum at the position of -1.0 d. The maximum value of the DCF is 0.98 ± 0.17. The centroid position corresponding to this peak is 0.4 d. To give a statistically reliable result, 1000 Monte Carlo simulations are performed. The CCPD is obtained and plotted in Figure 3. From it, the time lag and the uncertainties of $0.0^{+1.1}_{-1.0}$ d are derived.

The ZDCF is calculated and plotted in the bottom panel of Figure 2. The peak of $0.93^{+0.01}_{-0.01}$ is located at $0.0^{+0.7}_{-0.0}$ d. The centroid is 0.5 d. The results by the two methods are in good agreement with each other. This means that the variation in the B band is strongly correlated with that in the V band with a lead of about 0 d.
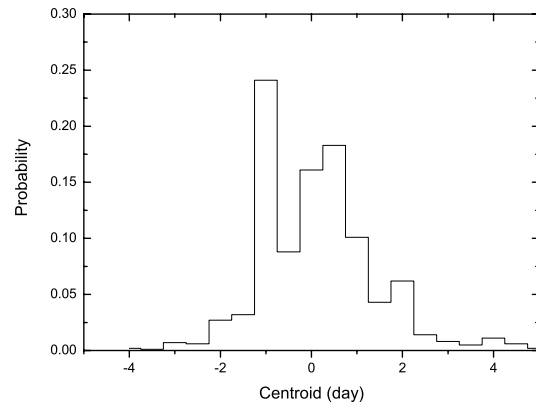
Fig. 3 Normalized CCPDs relative to the central peak obtained by running 1000 FR/RSS Monte Carlo simulations.
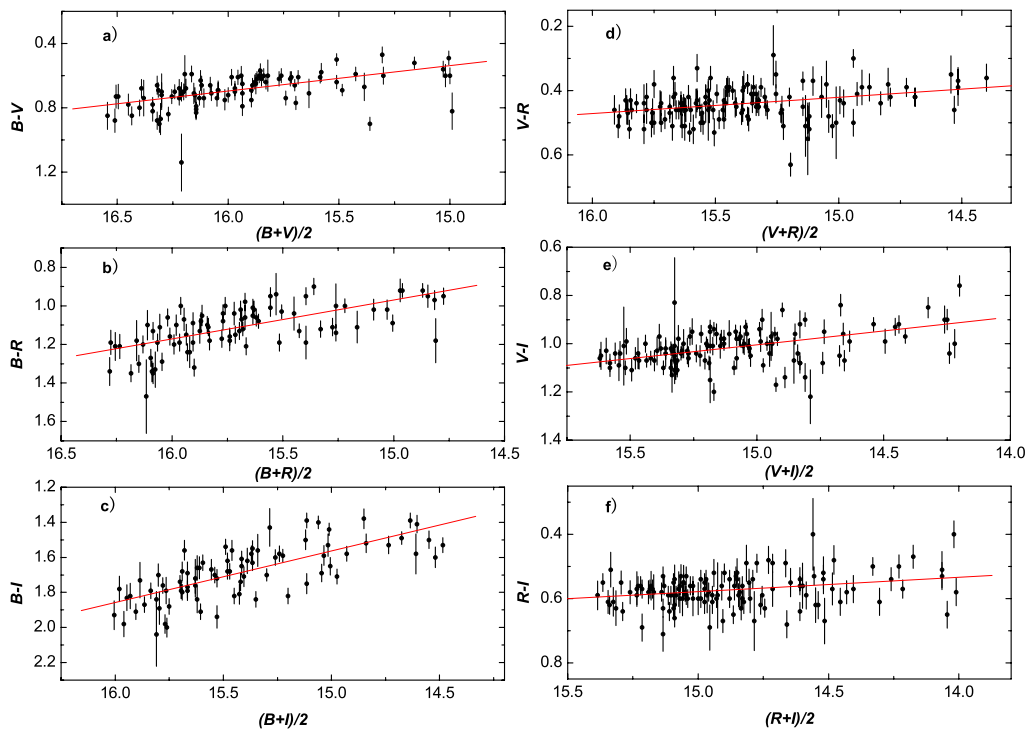
Fig. 4 Color index as a function of brightness. The lines are the best fits to the points.

This procedure is applied to each of the two bands of $BVRI$. The results are shown in Table 2. Col. (1) gives the band, Col. (2) the DCF peak, Col. (3) the DCF peak position, Col. (4) the centroid of the DCF, Col. (5) the ZDCF peak, Col. (6) the ZDCF peak position, and Col. (7) the centroid of the ZDCF. The results suggest the existence of significant correlations among $BVRI$ band light curves and no delays between their variations within the range of errors.

Table 2 DCF and ZDCF Results for Different Optical Bands

Band	DCF_{peak}	τ_{peak} (d)	$\tau_{centroid}$ (d)	$ZDCF_{peak}$	τ_{peak} (d)	$\tau_{centroid}$ (d)
$B-V$	0.98 ± 0.17	-1.0	$0.0^{+1.1}_{-1.0}$	$0.93^{+0.01}_{-0.01}$	$0.0^{+0.7}_{-0.0}$	0.5
$B-R$	0.91 ± 0.09	0.0	$0.4^{+0.6}_{-0.9}$	$0.95^{+0.01}_{-0.01}$	$0.1^{+0.7}_{-0.1}$	0.2
$B-I$	1.00 ± 0.20	1.0	$0.5^{+0.5}_{-1.0}$	$0.87^{+0.02}_{-0.02}$	$0.0^{+0.7}_{-0.0}$	0.1
$V-R$	0.92 ± 0.14	1.0	$0.5^{+0.5}_{-0.5}$	$0.93^{+0.01}_{-0.01}$	$0.1^{+0.6}_{-0.1}$	0.7
$V-I$	1.03 ± 0.21	1.0	$0.1^{+0.9}_{-0.6}$	$0.88^{+0.02}_{-0.02}$	$0.0^{+0.2}_{-0.0}$	1.4
$R-I$	0.95 ± 0.10	0.0	$0.0^{+0.5}_{-0.5}$	$0.90^{+0.02}_{-0.02}$	$-0.1^{+0.1}_{-0.7}$	0.3

4 COLOR INDEX

The existence of spectral changes possibly related to flux variations is investigated by analyzing color indexes. For the B and V bands, the color index and brightness are taken as $B-V$ and $(B+V)/2$ by coupling the data within 30 min intervals. The pairs without error bars and with zero lag (meaning no exact interval) are discarded. The variations of the color index $(B-V)$ with brightness are shown in Figure 4(a). The solid line in the figure shows the linear least-squares fit to the data points, which has a slope of 0.16. The Pearson correlation coefficient is 0.61, and the significance level is less than 10^{-4}, suggesting a strong correlation between color index and brightness. The relations between the color indexes of $B-R$, $B-I$, $V-R$, $V-I$, $R-I$ and the brightness are also investigated. The analysis of the other color indexes leads to similar results (see Fig. 4). The corresponding results are listed in Table 3. Cols. (1)–(5) represent the color index, the number of pairs, the slope, the correlation coefficient and the significance level, respectively. A clear bluer-when-brighter chromatism can be seen, in the sense that the spectrum steepens as the brightness decreases.

Table 3 Correlations between Color Index and Brightness

Color Index	N	Slope	r	Probs.
$B-V$	91	0.16 ± 0.01	0.61	$< 10^{-4}$
$B-R$	83	0.20 ± 0.01	0.68	$< 10^{-4}$
$B-I$	81	0.29 ± 0.01	0.74	$< 10^{-4}$
$V-R$	131	0.05 ± 0.01	0.33	$< 10^{-4}$
$V-I$	123	0.11 ± 0.01	0.49	$< 10^{-4}$
$R-I$	125	0.04 ± 0.01	0.29	0.01

5 DISCUSSION

In this analysis, it is found that the light curves in the four bands ($BVRI$) are well correlated. However, the lags between variations among different optical bands are not detected. Peterson et al. (1998) investigated the lags between UV and optical continuum variations in well-studied AGNs. They confirmed the existence of lags in NGC 7469, but did not find statistically significant interband continuum lags in NGC 5548, NGC 3783, or Fairall 9. For S5 0716+714, a good correlation was noticed between the light curves in the different optical passbands (Sagar et al. 1999), and an upper limit of the time lag of 0.0041 d between variations in the V and I bands was found by Qian et al. (2000). For BL Lacertae, the light curves in the different optical bands ($UBVRI$) are well correlated, but no significant, measurable time delays between the B and R bands were found (Villata et al. 2002). For the blazar AO 0235+164, Hagen-Thorn et al. (2008) found that the variations in the B

band lead those in the R band by $\sim$0.5–1 hr, while variations in the V and I bands are simultaneous within 0.5 hr with the variability in the R band. In addition, a 0.5$\pm$2.4 d lag was detected between B and V in the quasar MR2251–178 (Arévalo et al. 2008). For the Seyfert galaxy NGC 3783, the V and B band fluctuations were simultaneous within their time-resolution, with a delay of V behind B between –0.8 and 1.5 d (Arévalo et al. 2009). Bonning et al. (2009) studied the variability of the blazar 3C 454.3, and found an excellent correlation between the IR, optical, UV, and gamma-ray light curves with a time lag of less than one day. However, the X-ray flux is not correlated with either gamma-ray or longer wavelength data. The null or small time lags in optical regimes may be the result of very small frequency intervals, and may indicate that the photons in these wavelengths should be produced by the same physical process and emitted from the same spatial region.

According to the inhomogeneous jet models, time delays are expected between emissions in different energy bands, as plasma disturbances propagate downstream (Georganopoulos & Marscher 1998). Multi-wavelength monitoring of blazars shows that flares usually begin at high frequencies and then propagate to lower frequencies, implying that high-frequency synchrotron emission arises closer to the core than low-frequency synchrotron emission does (Ulrich et al. 1997; Marscher 2001). High energy electrons emit synchrotron radiation at high frequencies and then cool, emitting at progressively lower frequencies and resulting in time lags between high and low frequencies (Bai & Lee 2003). In addition, using the disk reprocessing model (Cackett et al. 2007), Breedt et al. (2009) estimated the lags between different optical bands in the Seyfert Galaxy Mrk 79. Their detected lags, except in the R band, were consistent with the expected ones. So, even small or null time lags between optical bands are expected due to the closeness of the two energy bands compared with the multi-wavelength output of the source. In this work, due to the limitation of the light-curve time resolution, lags on the order of minutes cannot be investigated. So, much denser monitoring data of this source are needed.

The result indicates a strong correlation between the color index and the brightness (see Fig. 4). The source became bluer when brighter. In other words, the spectrum became flatter when the object was brighter, and steeper when fainter. Vagnetti et al. (2003) analyzed light curves of eight BL Lac objects including OQ 530, and found that all of the objects tended to be bluer when brighter. To quantify the spectral variations, they also computed a parameter β representing the spectral slope changes per unit log-luminosity change (see Trèvese et al. 2002). OQ 530 had the highest value of β. Taking into account the value of the spectral slope α, this object showed variability and spectral properties still consistent with those of a BL Lac. OQ 530 is hosted by a relatively bright galaxy (Massaro et al. 2004), whose light may effect colors and color changes. The bluer-when-brighter trends were also observed by some authors for some BL Lac objects (D'Amicis et al 2002; Gu et al. 2006; Wu et al. 2007; Dai et al. 2009; Papadakis 2003), while there are a few objects showing a weak trend or the opposite trend (Fan & Lin 2000; Ciprini et al. 2007).

This common phenomenon may be explained in different ways (Fiorucci et al. 2004). It may indicate the presence of two components that contribute to the overall emission in the optical region, one variable (with a flatter slope), and the other stable. It is also possible to explain it with a one-component synchrotron model: the more intense the energy release, the higher the particle's energy. Moreover, it could also be explained if the luminosity increase was due to the injection of fresh electrons, with an energy distribution harder than that of the previous, partially cooled ones (Kirk et al. 1998; Mastichiadis & Kirk 2002). Another possible explanation for the observed spectral variation is the existence of a delay between different light curves: if the flux increases or decreases with the same rate in both light curves, but the variations at high frequency lead those at the low frequency, then the spectrum is bluer when the flux is rising. If the fluxes at different frequencies vary simultaneously, but the amplitude is larger at the higher frequency than at the lower one, the source shows a bluer-when-brighter chromatism (Wu et al. 2007; Papadakis et al. 2007). It has been found that the amplitude of the variations is systematically larger at higher frequencies (see Gu et al. 2007, and references therein).

In this case, no apparent time lag is found between variations in different wave bands. The bluer-when-brighter phenomenon may be mainly attributed to the larger amplitude variations at higher frequencies. From Table 1, one can see that σ and F_{var} of short-wave bands are larger than those of long-wave bands. Additionally, V is plotted as a function of B in Figure 5. The solid line is the best fit to the data. From it, one can derive that $V = (1.86 \pm 0.35) + (0.84 \pm 0.02)B$. This means that the higher the frequency, the larger the variation, which might cause the bluer-when-brighter phenomenon.
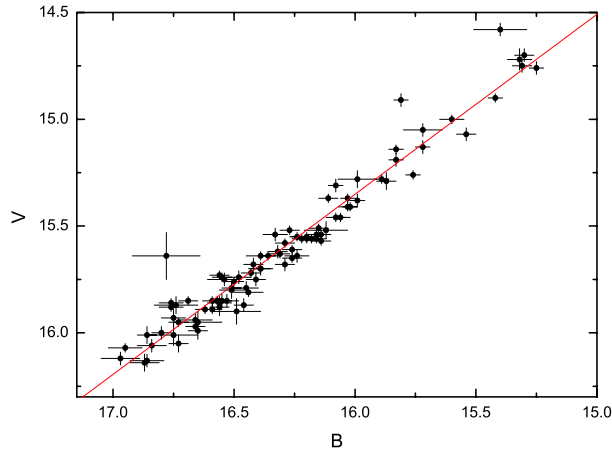
Fig. 5 Relation between B and V. The solid line is the best fit to the points.

6 CONCLUSIONS

The multi-band optical data are collected on the source of OQ 530. The variations between different optical bands have been analyzed, and the time lags and their uncertainties are convincingly determined for the first time. The results suggest that the variations are correlated very strongly with zero-lag. This means that the optical emission is dominated by the same physical mechanism. The correlation between the color index and magnitude shows that the brighter the source, the harder the spectrum, in the sense that the spectral slope flattens when the source luminosity increases.

References

Alexander, T. 1997, Astronomical Time Series, eds. D. Maoz, A. Sternberg, & E. M. Leibowitz, 1997 (Dordrecht: Kluwer), 163

Arévalo, P., Uttley, P., Kaspi, S., et al. 2008, MNRAS, 389, 1479

Arévalo, P., Uttley, P., Lira, P., et al. 2009, MNRAS, 397, 2004

Bai, J. M., & Lee, M. G. 2003, ApJ, 585, L113

Barbieri, C., Cristiani, S., & Romano, G. 1982, AJ, 87, 616

Blandford, R. D., & Königl, A. 1979, ApJ, 232, 34

Bonning, E. W., Bailyn, C., Urry, C. M., et al. 2009, ApJ, 697, L81

Breedt, E., Arévalo, P., McHardy, I. M., et al. 2009, MNRAS, 394, 427

Cackett, E. M., Horne, K., & Winkler, H. 2007, MNRAS, 380, 669

Carini, M. T., Miller, H. R., & Goodrich, B. D. 1990, AJ, 100, 347

Chatterjee, R., Jorstad, S. G., Marscher, A. P., et al. 2008, ApJ, 689, 79

Ciprini, S., Tosti, G., Raiteri, C. M., et al. 2003, A&A, 400, 487

Ciprini, S., Takalo, L. O., Tosti, G., et al. 2007, A&A, 467, 465

Dai, B. Z., Zhang, B. K., & Zhang, L. 2006, New Astronomy, 11, 471

Dai, B. Z., Li, X. H., Liu, Z. M., Zhang, B. K., et al. 2009, MNRAS, 392, 1181

D'Amicis, R., Nesci, R., Massaro, E. M., et al. 2002, PASA, 19, 111

Edelson, R. A., & Krolik, J. H. 1988, ApJ, 333, 646

Edelson, R., Turner, T. J., Pounds, K., et al. 2002, ApJ, 568, 610

Fan, J. H., & Lin, R. G. 2000, ApJ, 537, 101

Fiorucci, M., Ciprini, S., & Tosti, G. 2004, A&A, 419, 25

Fossati, G., Maraschi, L., Celotti, A., et al. 1998, MNRAS, 299, 433

Georganopoulos, M., & Marscher, A. P. 1998, ApJ, 506, L11

Ghosh, K. K., Ramsey, B. D., Sadun, A. C., et al. 2000, ApJS, 127, 11

Gu, M. F., Lee, C. U., Pak, S., et al. 2006, A&A, 450, 39

Gupta, A. C., Fan, J. H., Bai, J. M., & Wagner, S. J. 2008, AJ, 135, 1384

Hagen-Thorn, V. A., Larionov, V. M., Jorstad, S. G., et al. 2008, ApJ, 672, 40

Heidt, J., & Wagner, S. J. 1996, A&A, 305, 42

Kühr, H. 1977, A&AS, 29, 139

Kirk, J. G., Rieger, F. M., & Mastichiadis, A. 1998, A&A, 333, 452

Liu, Y., Li, J., & Fan, J. H. 2007, ChJAA (Chin. J. Astron. Astrophys.), 7, 380

Liu, H. T., Bai, J. M., Zhao, X. H., et al. 2008, ApJ, 677, 884

Marscher, A. P. 2001, ASPC, 224, 23

Marshall, K., Ryle, W. T., & Miller, H. R. 2008, ApJ, 677, 880

Massaro, E., Mantovani, F., & Fanti, R. 2004, A&A, 423, 935

Mastichiadis, A., & Kirk, J. G. 2002, PASA, 19, 138

Miller, H. R. 1978, ApJ, 223, L67

Papadakis, I. E., Villata, M., & Raiteri, C. M. 2007, A&A, 470, 857

Papadakis, I. E., Boumis, P., Samaritakis, V., et al. 2003, A&A, 397, 565

Peterson, B. M., Wanders, I., Horne, K., et al. 1998, PASP, 110, 660

Qian, B., Tao, J., & Fan, J. 2000. PASJ, 52, 1075

Raiteri, C. M., Villata, M., Aller, H. D., et al. 2001, A&A, 377, 396

Raiteri, C. M., Villata, M., Tosti, G., et al. 2003, A&A, 402, 151

Raiteri, C. M., Villata, M., Larionov, V. M., et al. 2008, A&A, 480, 339

Roy, M., Papadakis, I. E., Ramos-Colón, E., et al. 2000, ApJ, 545, 758

Sagar, R., Gopal-Krishna, Mohan, V., Pandey, A. K., et al. 1999, A&AS, 134, 453

Soldi, S., Türler, M., Paltani, S., et al. 2008, A&A, 486, 411

Stickel, M., Padovani, P., Urry, C. M., et al. 1991, ApJ, 374, 431

Stickel, M., Fried, J. W., & Kühr, H. 1993, A&AS, 98, 393

Tagliaferri, G., Ravasio, M., Ghisellini, G., Giommi, P., et al. 2003, A&A, 400, 477

Trèvese, D., & Vagnetti, F. 2002, ApJ, 564, 624

Ulrich, M. H., Maraschi, L., & Urry, C. M. 1997, ARA&A, 35, 445

Urry, C. M., & Padovani, P. 1995, PASP, 107, 803

Vagnetti, F., Trevese, D., & Nesci, R. 2003, ApJ, 590, 123

Villata, M., Raiteri, C. M., Kurtanidze, O. M., et al. 2002, A&A, 390, 407

Villata, M., Raiteri, C. M., Larionov, V. M., et al. 2009, A&A, 501, 455

Wu, J., Zhou, X., Ma, J., et al. 2007, AJ, 133, 1599